International Journal of Scientific & Engineering Research Volume 6, Issue l, %ÌÉÙÜÈÙà-2015
ISSN 2229-5518

Satellite Image Matching using Kalman Filter and a cross correlation technique

Wafaa Rajaa DRIOUA[1], Nacèra BENAMRANE[1], Noureddine KHELOUFI

Abstract— In this paper, we propose a method for evaluating the displacement and deformation fields for pair of multi temporal images, one before and one after deformation; based on a matchning technique of cross correlation. First, according to the noise present in the images and the long computation time, a denoising based on the Kalman filter and a multi-resolution analysis of effiient optimization scheme are proposed to improve the quality and speed time calculation. Second, an algorithm for matching based on the gray levels cross correlation is intoduced to improve the efficiency on matching. Our method was tested on satellite images and the results are encouraging.

Index Terms— Matching images, cross-correlation, displacement, deformation, satellite images.

1 Introduction

Optical techniques have opened up a wide field of applications in remote monitoring environments, mobile robotics, control or measurement. The objective of this paper is to develop a method to measure the displacement and deformation fields using the cross-correlation technique in gray levels. The general principle is based on matching images in computer vision. Two steps are required for any measure:

- The matching between the two multi temporal images is to determine a set of homologous pixels corresponding to the same physical point.
- The extent of the displacement field and the calculation of the deformation field between the two images (reference state and deformed state).

Several authors Vincent L., [1] Chambon S., [2] presented a classification of matching methods. The criteria used are generally the nature and dimension of attributes (constituting elements) to match, the field (local or global), the problem to solve, the constraints used, the measurement of similarity measure...

In recent years digital image correlation given by Peters W.H. et al [3] Chu T.C. et al [4] has become increasingly important. Many authors use the correlation Crouzil A. et al [5]. Zhao, F. et al [6] presented a method based on normalized cross-correlation that can effectively manage a pair of images with a big change and Rziza M. et al [7] presented algorithms for estimating disparity, based on the method of estimating a dense disparity map by using higher order statistics and robust correlation method. Due to the size of the data, matching can be very large, which is why several methods use a hierarchical of scheme matching like Qin, X. et al [8] who used a pyramid image and Fookes, C. et al [9] who presented extensions of the stereo matching based on mutual information and a approach with two hierarchical levels in order to increase the robustness of the algorithm. Also Hu Hao et al [10] presented a method of automatic vision to measure the deformation of surfaces. This method is based on image correlation and binocular stereovision. Pablo J. et al [11] proposed using a new method to measure the correlation of the deformation field. Finally, Guérin C. et al [12], use the digital surface models (DSMs) that create a geo-localized map of elevation changes of an urban scene from a set of couple images.

• [1] Departement of computer sciences, university of sciences and technology Mouhamed Boudiaf, Oran, Algeria.
Wafaa.drioua@univ-usto.dz, nacera.benamrane@univ-usto.dz

2 Description of the Matching Method

Ttwo images are used, the first is known as the reference image, the second is distorted. The steps of our approach are summarized in figure.1

2.1 Denoising by the Kalman filter

We will start by denoising step. The KALMAN filter Némesin V. [13] is a recursive estimator. It has two distinct phases:

A phase of prediction using the estimated state of the previous time to produce an estimate of the current state, the phase of updating the current observation of the state that is used to correct the predicted state in order to obtain a more accurate estimate.

```
For i=1 to nb_iteration do
 Kalman_{i,j} = prediction_{i,j}/(valrediction_{i,j} - bruit_{i,j});
 Correction_{i,j} = gain*prediction_{i,j} + (1-gain) * observation_{i,j} + kalman_{i,j} *(observation_{i,j} - prediction_{i,j});
Correction_var_{i,j} = prediction_var_{i,j} * (1- kalman_{i,j});
 Prediction_var_{i,j} = correction_var_{i,j};
 Prediction_{i,j} = Correction_{i,j};
End.
```

International Journal of Scientific & Engineering Research Volume 6, Issue l0i%ÌÉÙÜÈÙà-2015
ISSN 2229-5518

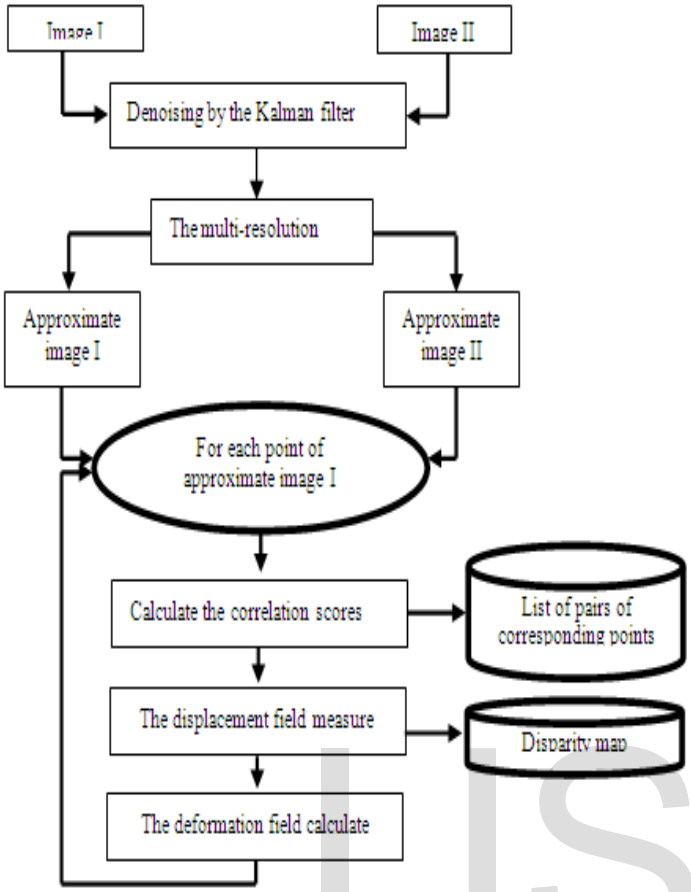

Fig. 1. Different steps of the approach

2.2 The Multi Resolution

A multi resolution approach was adapted; the model is based on a multi resolution wavelet decomposition obtained by Daubechies wavelets. Each multi temporal image is decomposed into three levels of resolution; we apply our approach on the level of coarsest resolution. Coupling with a multi resolution analysis allows a computational optimization while approaching the performance of the original method.

2.3 Image Matching

The principle of the digital image correlation is shown in fig2. Two images are not taken under the same lighting conditions, or with identical cameras. It is therefore necessary to achieve more than one simple correlation of gray levels.

2.3.1 Similarity Measure based on Correlation

The cross-correlation coefficient is used to calculate a normalized correlation factor, which comes down to not comparing the levels of gray but rather the way in which these levels of gray vary. In our approach, we use the MORAVEC measure (robust to noise) and the centred normalized cross correlation measure ZNCC (less expensive in computation time) Lane R A. et al [14].

$$ZNCC = \frac{(f_1 - \bar{f}_1) - (f_2 - \bar{f}_2)}{\left\| f_1 - \bar{f}_1 \right\|^2 \cdot \left\| f_2 - \bar{f}_2 \right\|^2}$$

$$MOR = \frac{2(f_1 - \bar{f}_1) - (f_2 - \bar{f}_2)}{\left\| f_1 - \bar{f}_1 \right\|^2 + \left\| f_2 - \bar{f}_2 \right\|^2}$$

f_i with i= 1,2 are vectors containing the pixel gray level of images 1 and 2.
$\bar{f}_i$ with i= 1,2 are the means.

After testing different window size correlations, we chose a window [7x7] with a search box dimension [17x17].

2.3.2 Correlation algorithm

Mi: the points of the first image.
Mj: the points of the second image.
F1: window of correlation centred on each point of the first image.
F2: window of correlation sliding on the second image
For each point Mi of image1 do
Center the window F1 on the point Mi
Choose an area of research in image2
For each point Mj of the search ZONE do:
Center the window F2 on the point Mj
Calculate correlation scores associated with the pixel Mi (Either by measurement or normalized cross-correlation centred or MORAVEC measurement).
Test the coefficient of maximum score
(The point Mi corresponding to Mj is one for which the score is greater).

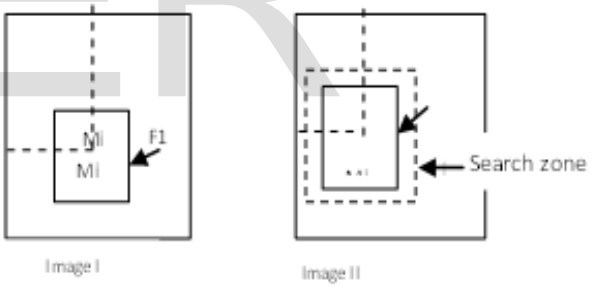

Fig. 2. Search for a match by correlation

The accuracy of displacement measurements depend on the performance of the correlation technique. Given the coordinates of the points in the original image and the coordinates of these physical points of the distorted image, obtained by cross-correlation technique, the displacement field and strain can be calculated.

2.4 The Measurement of the Displacement Fields

The deformations are estimated by a post treatment from displacement measure. After matching pairs of homologous points, the displacements are measured by subtracting the coordinates of the initial points and deformed.

$$\begin{cases} x^* = x + \Delta x \\ y^* = y + \Delta y \end{cases} \rightarrow \begin{cases} \Delta x = x^* - x \\ \Delta y = y^* - y \end{cases} \quad (1)$$

Thus, the displacement is represented by

$$\Psi(x) = \begin{pmatrix} \Delta x \\ \Delta y \end{pmatrix} \quad (2)$$

International Journal of Scientific & Engineering Research Volume 6, Issue l0%ÌÉÙÜÈÙà-2015
ISSN 2229-5518

In our method disparity at the point x is represented by the norm displacement vector at the point x (Euclidean distances).

2.5 The Calculation of the Deformation Fields

Now we describe the deformation model used. The state of deformation can be described by a tensor of deformation defined to any point. We talk of a deformation field. To deduce the deformation at a point, two approaches are used

2.5.1 Averaging of deformation of triangular elements in the vicinity:

The deformations of the considered point correspond to the average value of distortion of the triangular elements. There are two approaches as illustrated in figure. 3. The coefficients assigned to the elements of figure. 3 correspond to the value of the deformation of the triangular element.

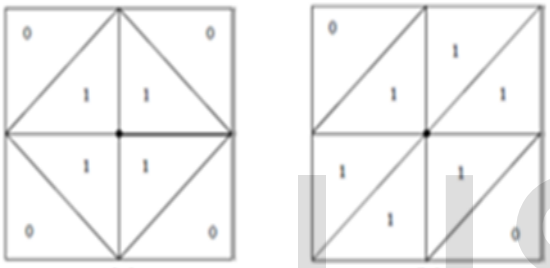

(a) (b)

Fig. 3. (a) Localized structure, (b) diagonal structure

Principle of calculation of the deformation of a triangular element:

Calculations of deformations are made on triangular elements, assuming that each triangle submitted a homogeneous deformation.

A change of reference must be effected in order to express the coordinates of the triangle points $(x_0 x_1 x_2)$. Changes in the reference are effected so that the point whose deformation we are trying to calculate is the origin of referee x_0, x_1 is on the x-axis and x_2 is on vertical axis. A point of initial coordinates (x_1, y_1) , in a homogeneous deformation will be coordinated (x_1^*, y_1^*) .

$[F]$ is a second order tensor called deformation gradient such that:

$$[F] = \begin{bmatrix} F_{11} & F_{12} \\ F_{21} & F_{22} \end{bmatrix} \quad (3)$$

Components (x_1^*, y_1^*) and (x_2^*, y_2^*) can be written as follows:

$$\begin{cases} x_1^* = F_{11}.x_1 + F_{12}.y_1 \\ y_1^* = F_{21}.x_1 + F_{22}.y_1 \end{cases} \quad (4)$$

And

$$\begin{cases} x_2^* = F_{11}.x_2 + F_{12}.y_2 \\ y_2^* = F_{21}.x_2 + F_{22}.y_2 \end{cases} \quad (5)$$

After solving the system

$$\begin{cases} x_1^* = F_{11}.x_1 + F_{12}.y_1 \\ y_1^* = F_{21}.x_1 + F_{22}.y_1 \\ x_2^* = F_{11}.x_2 + F_{12}.y_2 \\ y_2^* = F_{21}.x_2 + F_{22}.y_2 \end{cases} \quad (6)$$

$$F_{11} = \frac{y_2.x_1^* - y_1.x_2^*}{x_1.y_2 - x_2.y_1} \quad (7)$$

$$F_{12} = \frac{-(x_2.x_1^*) + x_1.x_2^*}{x_1.y_2 - x_2.y_1} \quad (8)$$

$$F_{21} = \frac{y_2.y_1^* - y_1.y_2^*}{x_1.y_2 - x_2.y_1} \quad (9)$$

$$F_{22} = \frac{-(x_2.y_1^*) - x_1.y_2^*}{x_1.y_2 - x_2.y_1} \quad (10)$$

From the deformation gradient tensor [F] the Cauchy-Green tensor is defined as:

$$[C] = [F][F]^T \quad (11)$$

In contrast to [F] which can be non-symmetric [C] is a symmetric tensor such that:

$$C_{11} = F_{11}^2 + F_{12}^2 \quad (12)$$

$$C_{12} = C_{21} = F_{11}.F_{21} + F_{12}.F_{22} \quad (13)$$

$$C_{22} = F_{21}^2 + F_{22}^2 \quad (14)$$

The Green-Lagrange tensor is given from [C] by

$$[E] = \frac{1}{2}.([F].[F]^T - [I]) \quad (15)$$

$$E_{11} = \frac{F_{11}^2 + F_{21}^2 - 1}{2} \quad (16)$$

$$E_{12} = \frac{F_{11}.F_{12} + F_{22}.F_{21}}{2} \quad (17)$$

$$E_{21} = \frac{F_{11}.F_{12} + F_{22}.F_{21}}{2} \quad (18)$$

$$E_{22} = \frac{F_{12}^2 + F_{22}^2 - 1}{2} \quad (19)$$

The principal deformations are given by:

$$\begin{cases} \varepsilon_I = \ln(E_{11} + E_{22} + \sqrt{(E_{11} + E_{22})^2 + (2.E_{12})^2}) + 1 \\ \varepsilon_{II} = \ln(E_{11} + E_{22} - \sqrt{(E_{11} + E_{22})^2 + (2.E_{12})^2}) + 1 \end{cases} \quad (20)$$

So deformations along the normal and tangent are represented

International Journal of Scientific & Engineering Research Volume 6, Issue l0%ÌÉÙÜÈÙà-2015
ISSN 2229-5518

by the vector $\begin{pmatrix} \varepsilon_I \\ \varepsilon_{II} \end{pmatrix}$.

The deformations at the point x are represented by the norm of the deformation vector at point x (Euclidean distances).

2.5.2 Centred finite differences

Deformations are calculated from displacement measure at 3 and 5 points.
Centred finite differences at 3 points:

$$\varepsilon = \frac{U^{n+1} - U^{n-1}}{2s} \tag{21}$$

Centred finite differences at 5 points:

$$\varepsilon = \frac{-U^{n+2} + 8U^{n+1} - 8U^{n-1} + U^{n-2}}{12s} \tag{22}$$

Where s is a constant representing the difference in position of adjacent points, and U^i their displacement.

3 The Experimental Results

We present an experimental result to see the deformation achieved in a multi temporal image pair.

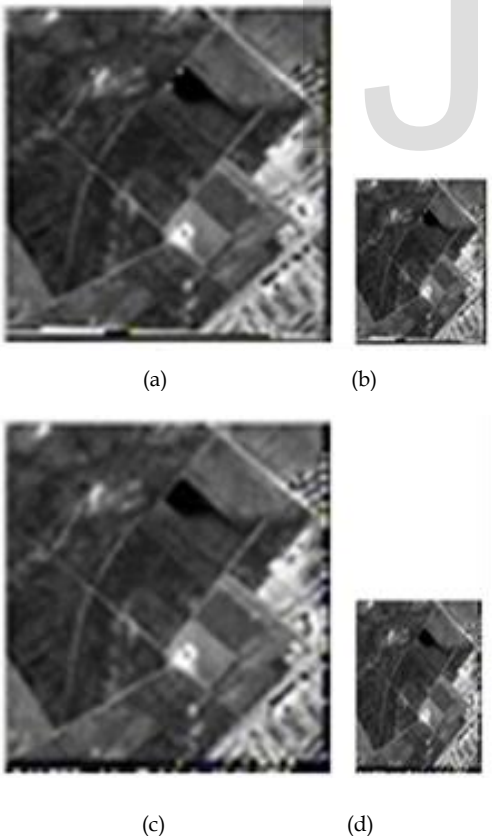

Fig. 4. The pair of original images (a,b), the pair of approximate images after the wavelet analysis (c,d).

Fig. 5. Disparity map using our method (a) with CCNC (b) with measurement of MORAVEC.

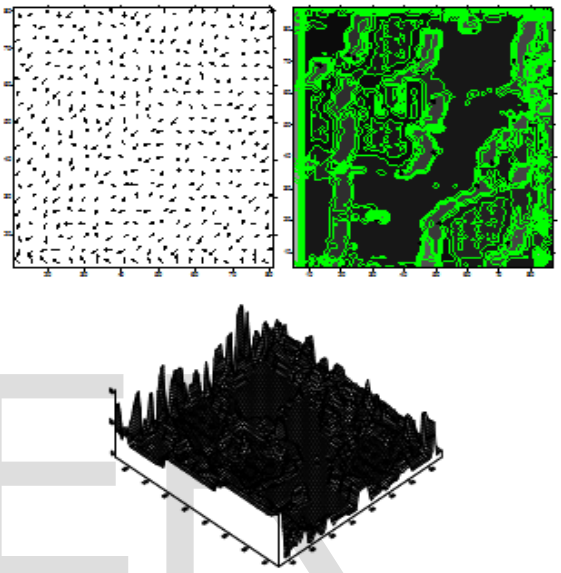

Fig. 6. Deformation field calculated by centred finite differences.

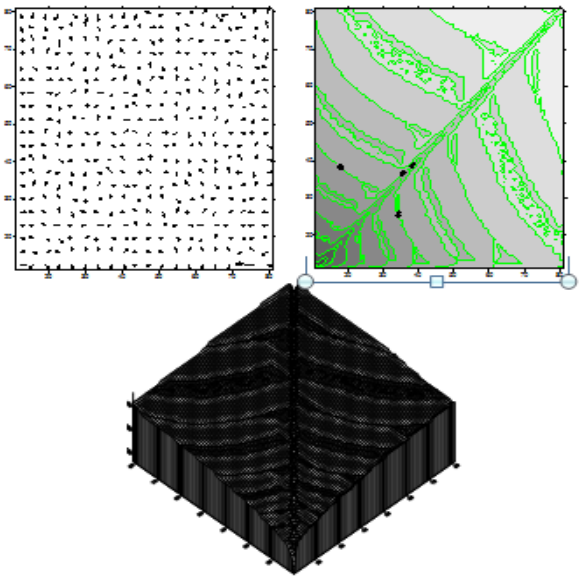

Fig.7. The deformation field calculated by the average strain of triangular elements of the localized structure.

International Journal of Scientific & Engineering Research Volume 6, Issue l0%ÌÉÙÜÈÙà-2015
ISSN 2229-5518

4 Conclusion

In this paper, we have presented a new method for matching based on the conservation of optical flow using a cross-correlation technique. These contributions are demonstrated and these performances are evaluated on real data.

We use a framework for effective minimization of both multi resolution and denoising. This efficient optimization scheme offers new perspectives for image matching applications. The multi resolution reduces the computation time without degrading the estimation of deformation since our approach is based on a dense matching technique.

We can draw multiple conclusions from this work:

- The correlation is an attractive means as it is accurate and sensitive, but the correlation coefficients require a very large computation time for their estimation; for this reason, a multi-resolution scheme was adopted.
- The approach allows both matching and an estimation of deformation at each point using a technique of dense matching.
- The analysis of the deformation field is used to detect and characterize changes.
- The deformations have been calculated according to the results of the correlation, based on the conservation of optical flow.
- Our method is suitable for finding the deformations including changes that are due to shots of the same scene spaced in time.
- Follow up in the use of this method will consist of work to be carried out at multiple resolution levels.

References

[1] Vincent, L., "Gestion des occultations en réalité augmentée," doctoral thesis, Honri Poincaré University. Nancy I, 2001.

[2] Chambon, S., "Mise en correspondence stéréoscopique d'images couleur en présence d'occultations," doctoral thesis. University of Toulouse III, 2005.

[3] Peters W. H. and Ranson W. F.," Digital imaging techniques in experimental stress analysis," Opt. Eng, vol. 21, pp. 427-431, 1982.

[4] Chu T. C., Ranson W. F. and Sutton M. A.,"Applications of digital image-correlation techniques to experimental mechanics," Exp. Mech, pp. 232-245, 1985.

[5] Crouzil A., Chambon S., "Mesures de corrélation pour des images couleur," Institute for Research in Computer Science of Toulouse. Paul Sabatier University, 2005.

[6] Zhao F., Huang H., Gao W., "Image matching by normalized cross-correlation," IEEE ICASSP, vol. 2, pp. 729-732, 2006.

[7] Rziza M., Aboutajdine D., Mrin L. and Tamtaoui A., "Schèma multi résolution d'un champ de disparité dense sous contrainte epipolaire pour les images bruitées," Colloques sur le Traitement du Signal et des Images GRETSI, 2001.

[8] Qin X., Li Li. And Tian, S., "A new image matching algorithm with modified greedy algorithm for remote sensing imagery," ISPRS Workshop on Service and Application of Spatial Data Infrastructure, Hangzhou, China, 2003.

[9] Fookes C., Bennaoun A. and Lammna A., "Improved stereo image matching using mutual information and hierarchical prior probabilities," IEEE Pattern Recognition, vol. 2, pp. 937-940, 2002.

[10] Hu Hao, Liang Jin, Liu Jianwei, Xiao Zhenzhong and Tang Zhengzong, "Three-dimensional Deformation Measuring System Based on Vision Method," International Conference on Mechanical and Electrical Technology (ICMET), 2010.

[11] Pablo J., González M., Stramondo S. and Fernández J., "Coseismic Horizontal Offsets andFault -Trace Mapping Using Phase Correlation of IRS Satellite Images: The 1999 Izmit (Turkey) Earthquake," IEEE Transactions on geosciences and remote sensing, vol. 48, pp. 2242-225, 2010.

[12] Guérin C., Binet R. and Pierrot-Deseilligny M., "Détection des changements d'élévation d'une scène par imagerie satellite stéréoscopique," Article published in "RFIA (Pattern Recognition and Artificial Intelligence) Lyon, France, 2012.

[13] Némesin V., "Estimation robuste du filtre de Kalman couple," GSM Team, Fresnel Institute (UMR 6133). Saint Jérôm University, 2007.

[14] Lane R A., Thacker N A. and N L Seed., "Stretch-correlation as a real-time alternative to feature-based stereo matching algorithms," Image and Vision Computing, vol. 12, pp. 203-212.